

# A Boundary Layer Analysis for the Initiation of Reactive Shear Bands

Robert Timms<sup>a\*</sup>, Richard Purvis<sup>a</sup>

<sup>a</sup>*School of Mathematics, University of East Anglia, Norwich NR4 7TJ;*

<sup>\*</sup>*Now at Mathematical Institute, University of Oxford, Oxford OX2 6GG;*

Email: timms@maths.ox.ac.uk

**Abstract:** A one-dimensional model for the initiation of shear bands in a reactive material is developed, which accounts for thermal softening, strain hardening and strain rate effects, and models the chemical reaction using an Arrhenius source term. An inhomogeneity in the heat flux is used as the stimulus for localised plastic deformation, and a solution is sought as a perturbation to the elastic solution. In the analysis, the thin zone of localisation is identified as a boundary layer. It is found that the behaviour of the perturbations to the temperature, stress and strain hardening variable in the localisation zone are governed by four dimensionless parameters which are known in terms of various material properties including density, heat of reaction, strain-rate sensitivity, thermal sensitivity and strain sensitivity. The resulting equations are solved numerically and a criterion for the onset of shear banding is discussed. The analysis highlights key physical properties which control the reactive shear banding process and gives a deeper insight into how such a process may be understood as a mechanism for the accidental ignition of reactive materials.

**Subject:** Mathematics

**Keywords:** Boundary Layer, Asymptotic, Shear Band, Reactive Materials

## 1 Introduction

The phenomenon of shear banding, where the flow of a material localises to narrow bands, is well-studied in a general context, often with a particular focus on metals [1–9], or granular and geological materials [10–13]. However, there have been comparatively few studies on the development of shear bands in reactive materials. A comprehensive review of the modelling of shear bands in inert materials can be found in [2]. Examples of shear band models developed specifically for explosive materials are less common in the literature, and are most often concerned with how the addition of a chemical heat source term affects the tendency for a shear band to form [14–16].

In particular, shear localisation is often suggested as a potential accidental ignition mechanism in explosive materials [14–21], backed up by experimental evidence (e.g. [22, 23]). It is suggested that shear banding could be a so-called ‘hot spot’ mechanism. It is widely accepted that when explosive materials are subject to unintended low energy mechanical stimuli, ignition is caused by localised regions of high temperature known as hot spots [22, 24]. Understanding the response of explosive materials to mechanical stimuli, and in particular understanding the mechanisms which cause the formation of such hot spots, is of key importance

in developing and maintaining safe procedures for working with and storing explosives.

The majority of models of shear banding are one-dimensional, owing to the large aspect ratio observed in experiments. A one-dimensional model which aimed to address the likelihood of both friction and shear banding as accidental ignition mechanisms is developed in [19]. The model predicts the existence of a maximum obtainable temperature in the absence of reaction, which depends on the pressure and shear velocity. Upon introduction of chemical heating, the shear rate required to achieve a thermal explosion decreases rapidly as the pressure increases. The model can track the developing shear band, but requires numerical solution to determine the velocity profile across the sheared layer. A more simple model, which considers the shear band as a localised region of uniform straining, is developed in [14]. The work extends the so-called Frank-Kamenetskii analysis [25], which describes the process of self-ignition, to account for mechanical heating. The stability of the steady shear banding solution is studied, and predictions for the maximum temperature at the centre of the band as a function of the plastic work are made. The analysis demonstrates how the mechanical process of shear banding may combine with the thermochemical process of self-ignition to increase the mechanical sensitivity of explosive materials. Caspar and Powers [15, 16, 26] studied a thin-walled, cylindrical, rigid-plastic specimen of the explosive material LX-14. Experimental studies were performed on an inert simulant, Mock 900-20, in order to characterise the effects of strain and strain-rate hardening. Their studies go on to use both numerical and analytical techniques to study how an inhomogeneity in the sample thickness can trigger the onset of a shear band. Further, shear localisation in LX-14 was shown to be sensitive to changes in mechanical properties, specific heat and activation energy, but relatively insensitive to changes in the thermal conductivity and kinetic rate constant.

In this paper we present a boundary layer analysis to describe the onset of shear localisation in a reactive material. Thermal softening effects play a key role in the initiation and development of shear bands, and so it is reasonable to assume that the additional heating due to chemical reactions occurring in the material will affect the rate of plastic work, which in turn increases the tendency for a shear band to form. Models of shear localisation in reactive materials typically resort to numerical solution (e.g. [16, 27]). However, in [15] a so-called “Thermal Explosion Theory” is developed for a rigid-plastic material under the assumption that most variables are spatially homogenous. This allows for the identification of three distinct periods: an induction stage, a reaction stage and a post-reaction stage. In the initial stage the plastic work, which is assumed spatially homogenous, causes the temperature to increase to that required for a significant reaction. The process then enters the reaction stage, in which heating due to chemical reaction dominates. Once the reaction has reached completion, the process enters the final stage where the temperature increase is dominated by plastic work once again. Estimates for the induction time are given from this approximate theory, and from a more rigorous asymptotic analysis where the strain hardening parameter takes on special values corresponding to no strain hardening and a linear dependence of stress with strain [15]. In the asymptotic analysis the large activation energy is exploited in order to determine the perturbation to the temperature. While the analysis provides useful estimates for the induction, it decouples the mechanical and chemical effects, and therefore does not account for the way in which heating due to chemical reaction affects the material behaviour during the so-called induction stage.

Here, we exploit the large activation energy in conjunction with the asymptotic analysis of inert shear bands in [8] in order to develop an asymptotic theory for shear bands which accounts for the effects of heating due to mechanical dissipation and chemical reaction simultaneously. In Section 2 we present the governing equations

for a one-dimensional model for reactive shear bands, taking into account thermal softening, strain hardening and strain-rate effects. In order to model the strain hardening behaviour, we propose a novel extension to the constitutive law used in [8]. The function for the plastic strain-rate takes an exponential form which is particularly convenient for the asymptotic analysis that follows.

The governing equations are recast in non-dimensional form using a thermal length scale, which is typically much shorter than the sample width. This allows us to make the simplifying assumption that the edges of the sample are effectively an infinite distance from the shear band, consistent with the physical observation that the shear band width is typically much smaller than the size of the slab. Motivated by [8] we use an inhomogeneity in the heat flux as the stimulus for localised plastic deformation, and treat the problem as a perturbation to the elastic solution.

In Section 3 the thin zone of localisation is treated as a boundary layer, and scalings for the plastic strain-rate and activation energy are introduced. The solution for the early-time elastic stage is given analytically in terms of the imposed heat flux inhomogeneity. The asymptotic analysis reduces the problem to a system of coupled nonlinear equations which govern the perturbations to the temperature, stress and strain hardening variable in the band. These are solved in conjunction with an auxiliary equation which determines a critical reaction timescale. In Section 4 the equations from the boundary layer analysis are expressed in terms of four new non-dimensional parameters. The results are compared with the inert case [8] and a criterion for the initiation of reactive shear bands is discussed. In Section 5 we compare the results of our asymptotic analysis with numerical results obtained using the the so-called “cohesive scheme” described by Zhou et al. [7]. We also consider an approximate solution, more akin to the Thermal Explosion Theory [15], which splits the problem into distinct plastic and reaction stages. It is demonstrated that accounting for the reaction in the early stages of the shear banding process is important in accurately determining the time to thermal runaway. We conclude in Section 6 and make some comments on the possible implications of this study.

## 2 Reactive Shear Band model

We consider a two-dimensional slab of explosive material of height  $2L$  subject to an applied uniform shearing motion, see Figure 1. The sample is loaded at time  $\tilde{t} = 0$  such that the constant velocity at  $\tilde{y} = \pm L$  is  $\pm \tilde{v}_0$ . In the absence of any inhomogeneity in the material properties, or in the initial or boundary conditions, it is assumed that the velocity profile is linear for  $-L < \tilde{y} < L$ . However, perturbations may be introduced which will allow for localisation to occur. For now, it is assumed that such perturbations will be uniform in the direction of shearing so that a one dimensional model is appropriate. The explosive material is assumed to behave as an elastic-plastic (e.g. [23]), with a constitutive law which accounts for strain hardening, strain-rate sensitivity and thermal softening effects. The heating of the material due to plastic work is modelled, as well as the subsequent self-heating due to exothermic reaction. The reaction is modelled using a one-step Arrhenius law which, though simple, is well known to give the correct qualitative behaviour (e.g. [14, 16, 28, 29]) and is able to well predict ignition times over several orders of magnitude in time (see [15] and references therein).

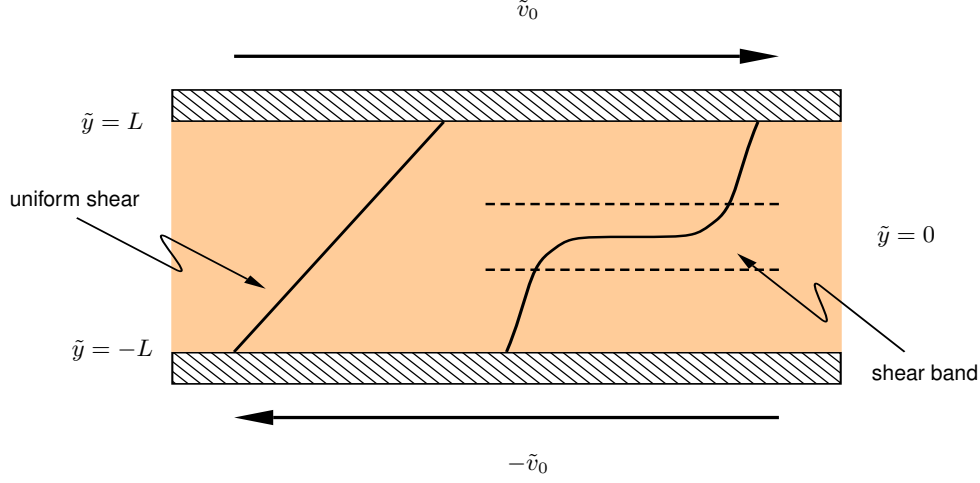


**Figure 1:** Schematic of uniform shearing vs. a shear band centered about  $\tilde{y} = 0$ .

In dimensional form the governing equations read:

$$\rho \tilde{v}_{\tilde{t}} = \tilde{s}_{\tilde{y}}, \quad \text{momentum balance;} \quad (2.1)$$

$$\rho c \tilde{T}_{\tilde{t}} = \kappa \tilde{T}_{\tilde{y}\tilde{y}} + \beta \tilde{s} \dot{\Gamma} + \rho \Omega A \exp(-E/(R\tilde{T})), \quad \text{energy balance;} \quad (2.2)$$

$$\tilde{s}_{\tilde{t}} = G(\tilde{v}_{\tilde{y}} - \dot{\Gamma}), \quad \text{elastic relationship;} \quad (2.3)$$

$$\dot{\Gamma} = \dot{\Gamma}(\tilde{s}, \tilde{T}, \Gamma), \quad \text{plastic flow law;} \quad (2.4)$$

$$\Gamma = \int_0^{\tilde{t}} \dot{\Gamma}(t') dt', \quad \text{plastic strain.} \quad (2.5)$$

Here the dependent variables are velocity  $\tilde{v}(\tilde{y}, \tilde{t})$ , stress  $\tilde{s}(\tilde{y}, \tilde{t})$ , temperature  $\tilde{T}(\tilde{y}, \tilde{t})$ , and plastic strain rate  $\dot{\Gamma}(\tilde{y}, \tilde{t})$ . The plastic strain  $\Gamma(\tilde{y}, \tilde{t})$  is determined by integration of strain rate. The material constants  $\rho$ ,  $G$ ,  $c$ ,  $\kappa$ ,  $\beta$ ,  $\Omega$ ,  $A$ ,  $E$  and  $R$ , are the density, elastic shear modulus, specific heat, thermal conductivity, Taylor-Quinney coefficient, heat of reaction, rate constant, activation energy and molar gas constant, respectively.

On the top and bottom of the slab we impose a fixed shearing velocity and assume an isothermal boundary condition, with appropriate compliance of the stress. The initial conditions are taken to correspond to the uniform shearing solution. Together they read

$$\tilde{v}(\pm L, \tilde{t}) = \pm \tilde{v}_0, \quad \tilde{T}(\pm L, \tilde{t}) = \tilde{T}_0, \quad (2.6)$$

$$\tilde{v}(\tilde{y}, 0) = \omega \tilde{y}, \quad \tilde{s}(\tilde{y}, 0) = \tilde{s}_0, \quad \dot{\Gamma}(\tilde{y}, 0) = \omega, \quad \Gamma(\tilde{y}, 0) = 0, \quad \tilde{T}(\tilde{y}, 0) = \tilde{T}_0, \quad (2.7)$$

where  $\omega$  is the nominal strain-rate. Specification of an initial stress  $\tilde{s}_0 > 0$  corresponds to starting the physical problem nearer to the onset of plastic deformation [8].

In order to initiate a shear band it is necessary to introduce some external localised stimulus. For this we consider an inhomogeneity in the heat flux placed at  $\tilde{y} = 0$  as in [8], introduced as

$$\kappa \tilde{T}_{\tilde{y}}(0^-, \tilde{t}) = -\kappa \tilde{T}_{\tilde{y}}(0^+, \tilde{t}) = Q(\tilde{t}) \geq 0, \quad \tilde{t} > 0, \quad (2.8)$$

where  $\kappa$  is the thermal conductivity and  $Q(\tilde{t})$  is assumed to be of small magnitude and short duration. Other choices for the stimulus for shear band initiation are available (e.g. [4, 9, 15, 16]), and similar analyses to the boundary layer analysis we will present could be conducted regardless of the choice of stimulus. Instead of considering an inhomogeneity in one of the model variables, such as temperature or strain-rate, or in the material properties, such as yield stress, we could instead make the ad-hoc assumption that the material is subject to a constant rate of average strain, and comprises a thin zone in which all of the heat generation takes place [30]. In the model developed in [30], a so-called weak zone is identified, to which all plastic deformation is confined. Owing to the zone's thinness, it is treated as a plane of uniform heat generation, which drives thermal softening behaviour in the material.

For the plastic strain-rate we propose an extension to the constitutive law used in [8], which takes into account thermal softening, strain hardening and strain-rate dependence. Strain hardening effects have been shown to be important in polymer bonded explosives, and are included in a number of models for reactive shear bands [15, 16]. The strain hardening behaviour of a range of explosive simulants, including cure cast, melt cast, and pressed formulations, can be found in [26]. The plastic strain-rate takes the following exponential form

$$\dot{\Gamma}(\tilde{s}, \tilde{T}, \Gamma) = \dot{\Gamma}^* \exp\{-[B_1^{-1}(\tilde{T}_p - \tilde{T}) + B_2^{-1}(\tilde{s}_p - \tilde{s}) + B_3^{-1}\Gamma]\}, \quad (2.9)$$

where  $\dot{\Gamma}^*$  is a dimensional reference strain-rate, and the constants  $\tilde{T}_p$  and  $\tilde{s}_p$  are the critical values of temperature and stress below which the plastic strain-rate is exponentially small. It is required that  $\tilde{T}_p > \tilde{T}_0$  and  $\tilde{s}_p > \tilde{s}_0$  so that the problem is started in the elastic stage in which plastic strain is initially negligible. The parameters  $B_1$ ,  $B_2$  and  $B_3$  are related to strain-rate sensitivity  $M$ , thermal sensitivity  $P$  and strain sensitivity  $N$  via the definitions

$$M \equiv \frac{1}{\tilde{s}_p} \frac{\partial \tilde{s}}{\partial \log \dot{\Gamma}} = \frac{B_2}{\tilde{s}_p}, \quad P \equiv -\frac{\tilde{T}_p}{\tilde{s}_p} \frac{\partial \tilde{s}}{\partial \tilde{T}} = \left( \frac{B_2}{\tilde{s}_p} \right) / \left( \frac{B_1}{\tilde{T}_p} \right), \quad N \equiv \frac{\dot{\Gamma}^* t^*}{\tilde{s}_p} \frac{\partial \tilde{s}}{\partial \Gamma} = \left( \frac{B_2}{\tilde{s}_p} \right) / \left( \frac{B_3}{\dot{\Gamma}^* t^*} \right), \quad (2.10)$$

where  $t^*$  is a reference time scale. This strain-rate model is a very close approximation of more typically adopted power law models (see [31] for a comparison), but offers a form which is much more convenient for the boundary layer analysis to follow.

We introduce non-dimensional variables, which are related to the dimensional variables by

$$t = \tilde{t}/t^*, \quad y = \tilde{y}/l, \quad v = \tilde{v}/\tilde{v}_0, \quad s = \tilde{s}/\tilde{s}_0, \quad \dot{\gamma} = \dot{\Gamma}/\dot{\Gamma}_0, \quad T = \tilde{T}/\tilde{T}_0, \quad q = Q/q_0,$$

and the parameters

$$\begin{aligned} t^* &= \frac{\tilde{s}_0}{G\dot{\Gamma}_0}, \quad l = \left( \frac{\kappa \tilde{s}_0}{\rho c G \dot{\Gamma}_0} \right)^{1/2}, \quad \dot{\Gamma}_0 = \frac{\tilde{v}_0}{l}, \quad \Gamma_0 = t^* \dot{\Gamma}_0, \quad \hat{\omega} = \frac{\omega}{\dot{\Gamma}_0}, \\ \hat{\rho} &= \frac{\kappa \dot{\Gamma}_0}{c \tilde{s}_0}, \quad \lambda = \frac{\beta \tilde{s}_0^2}{\rho c G \tilde{T}_0}, \quad \hat{E} = \frac{E}{R \tilde{T}_0}, \quad \hat{\Omega} = \frac{\Omega}{c \tilde{T}_0}, \quad \hat{A} = A t^*, \quad q_0 = \frac{\kappa \tilde{T}_0}{l}. \end{aligned} \quad (2.11)$$

The choice of the thermal length scale  $l \ll L$  places the rigid boundaries at  $y = \pm L/l$ . We choose to exploit the physical observation that shear bands are typically very thin compared with the sample size, taking the limit  $L/l \rightarrow \infty$  so that the material sample occupies the space  $-\infty < y < \infty$  [8].

To fix ideas we consider the values of various material properties for LX-14, which are typical of a wide

range of explosives [15, 26]. Using parameter values found in [15, 27, 32–34], we have  $\rho = 1.849 \times 10^3 \text{ kg m}^{-3}$ ,  $G \approx 3 \times 10^9 \text{ kg m}^{-1} \text{ s}^{-2}$ ,  $c = 1.130 \times 10^3 \text{ J kg}^{-1} \text{ K}^{-1}$ ,  $\kappa = 4.390 \times 10^{-1} \text{ W m}^{-1} \text{ K}^{-1}$ ,  $M \approx 0.1$ ,  $N \approx 0.1$ ,  $P \approx 1$ ,  $\beta = 1$ ,  $\omega = 10^3 \text{ s}^{-1}$ ,  $L = 3.47 \times 10^{-3} \text{ m}$ ,  $\tilde{T}_0 = 3 \times 10^2 \text{ K}$ ,  $\tilde{s}_0 \approx 4 \times 10^7 \text{ kg m}^{-1} \text{ s}^{-2}$ ,  $\Omega = 5.950 \times 10^6 \text{ J kg}^{-1}$ ,  $A = 5 \times 10^{19} \text{ s}^{-1}$ ,  $E = 2.206 \times 10^5 \text{ J mol}^{-1}$  and  $R = 8.314 \text{ J mol}^{-1} \text{ K}^{-1}$ . Choosing a representative strain-rate based on the thermal length scale  $l$  gives an extremely high value of  $\dot{\Gamma}_0 \sim 10^9 \text{ s}^{-1}$ . While this may be typical of the strain-rate in a fully-formed band (e.g. [7]), a more typical value of the strain-rate found within a developing shear band would be in the range  $\dot{\Gamma}_0 \sim 10^3$  to  $10^6 \text{ s}^{-1}$  [2, 7, 8]. In [8, 9] the scaling for the strain-rate is selected to be representative of that within a shear band, and is independent from the length scale. Varying  $\dot{\Gamma}_0$  between  $10^3$  and  $10^6 \text{ s}^{-1}$  gives the following order of magnitude estimates for the parameters:

$$\begin{aligned} t^* &\sim 10^{-9} \text{ to } 10^{-6} \text{ s}, \quad l \sim 10^{-9} \text{ m}, \quad \Gamma_0 \sim 10^{-2}, \quad \hat{\omega} \sim 10^{-4} \text{ to } 1, \quad \hat{\rho} \sim 10^{-7} \text{ to } 10^{-4}, \\ \lambda &\sim 10^{-3}, \quad \hat{E} \sim 10^2 \text{ to } 10^3, \quad \hat{\Omega} \sim 10, \quad \hat{A} \sim 10^{10} \text{ to } 10^{14}, \quad q_0 \sim 10^{11}. \end{aligned} \quad (2.12)$$

In the following boundary layer analysis we will exploit this freedom in choosing our scaling for the strain-rate in order to achieve the designated scalings for some of our non-dimensional parameters.

The non-dimensional governing equations for the shearing problem in the upper-half plane read

$$\hat{\rho} v_t = s_y, \quad (2.13)$$

$$T_t = T_{yy} + \lambda s \dot{\gamma} + \hat{\Omega} \hat{A} \exp(-\hat{E}/T), \quad (2.14)$$

$$s_t = v_y - \dot{\gamma}, \quad (2.15)$$

$$\dot{\gamma} = \frac{\dot{\Gamma}_0^*}{\dot{\Gamma}_0} \exp \left\{ - \left[ \frac{\tilde{T}_0}{B_1} (T_p - T) + \frac{\tilde{s}_0}{B_2} (s_p - s) + \frac{\Gamma_0}{B_3} \gamma \right] \right\}, \quad (2.16)$$

$$\gamma = \int_0^t \dot{\gamma}(t') dt', \quad (2.17)$$

where  $T_p = \tilde{T}_p/\tilde{T}_0 > 1$  and  $s_p = \tilde{s}_p/\tilde{s}_0 > 1$  are the non-dimensional critical temperature and stress, respectively.

### 3 Boundary layer analysis

We seek a solution of (2.13)–(2.16) in the form of a perturbation to the elastic ( $\dot{\gamma} = 0$ ) solution. In the following analysis, a thin zone centred around  $y = 0$  in which significant plastic work and reaction take place is identified. Outside of this region both the heating due to plastic work and heating due to reaction are exponentially small, and far from the centre of the localisation zone the elastic solution remains valid. The solution in the thin zone around  $y = 0$  is matched on to the elastic solution via an intermediate diffusive zone. Figure 2 shows a sketch of the asymptotic structure used in our boundary layer analysis.

By differentiating (2.13) with respect to  $y$  and integrating the result with respect to  $t$  we obtain an expression for  $v_y$  in terms of the stress. This is substituted into the elastic relationship (2.15) to give a single

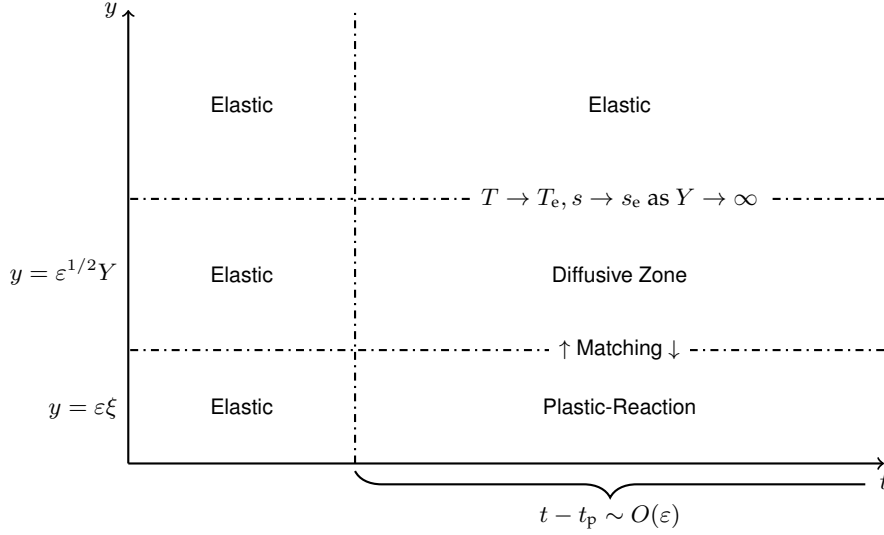


**Figure 2:** Sketch of the asymptotic structure used in to determine the equations governing the temperature, stress and plastic strain within the shear band. Three spatial regions are identified: the inner region, which corresponds to the shear band zone; the outer diffusive zone, which is used to match on to the elastic solution in the far-field; and the elastic zone. The analysis identifies two regimes in time: the early-time elastic solution; and the plastic-reaction stage, during which the material is heated by both plastic work and chemical reaction.

equation relating the stress and strain-rate. The governing equations then read

$$s_t = \hat{\rho}^{-1} \int_0^t s_{yy}(y, t') dt' + \hat{\omega} - \dot{\gamma}, \quad (3.1)$$

$$T_t = T_{yy} + \lambda s \dot{\gamma} + \hat{\Omega} \hat{A} \exp(-\hat{E}/T), \quad (3.2)$$

where the velocity has been eliminated using the initial condition  $v(y, 0) = \hat{\omega}y$ . The plastic strain-rate is still given by (2.16). Owing to symmetry considerations, we treat only the upper half plane, and solve the governing equations subject to the initial and boundary conditions

$$s(y, 0) = 1, \quad T(y, 0) = 1, \quad (3.3)$$

$$s_y(0, t) = 0, \quad T_y(0, t) = -q(t), \quad T(\infty, t) = 1. \quad (3.4)$$

In order to proceed with the boundary layer analysis, we must identify a small parameter  $\varepsilon$ . This is introduced through the ratios  $B_1/\tilde{T}_0$  and  $B_2/\tilde{s}_0$  by the relations

$$\frac{B_1}{\tilde{T}_0} = \beta_1^{-1} \varepsilon, \quad \frac{B_2}{\tilde{s}_0} = \beta_2^{-1} \varepsilon, \quad \frac{B_3}{\Gamma_0} = \beta_3^{-1} \varepsilon^{1/2}, \quad 0 < \varepsilon \ll 1, \quad (3.5)$$

where  $\beta_1$ ,  $\beta_2$  and  $\beta_3$  are  $O(1)$  constants. Such a scaling is typical of materials which exhibit shear banding [8]. It is assumed that the plastic strain-rate function can be multiplicatively scaled [8], so that  $\dot{\Gamma}^*/\dot{\Gamma}_0 = \dot{\gamma}_0 \varepsilon^{-1/2}$ , and the plastic strain-rate takes the non-dimensional form

$$\dot{\gamma}(s, T, \gamma) = \dot{\gamma}_0 \varepsilon^{-1/2} \exp\{-\varepsilon^{-1}[\beta_1(T_p - T) + \beta_2(s_p - s)] - \varepsilon^{-1/2}\beta_3\gamma\}. \quad (3.6)$$

where  $\dot{\gamma}_0$  is  $O(1)$ . The non-dimensional parameter  $\hat{\rho} = \kappa \dot{\Gamma}_0 / c \tilde{s}_0$  is typically small in materials which exhibit shear banding effects; for LX-14 we find  $\hat{\rho} \sim 10^{-2}$ . In order to take advantage of this, we introduce the scaling  $\hat{\rho} = \varepsilon \hat{\rho}_0$ , where  $\hat{\rho}_0$  is  $O(1)$ .

The largeness of the product of the pre-exponential factor  $\hat{A}$  and heat of reaction  $\hat{\Omega}$  is also exploited by setting

$$\hat{\Omega} \hat{A} = \hat{A}_0 \hat{E}^{1/2} T_R^{-1} \exp(\hat{E}/T_R), \quad (3.7)$$

where  $T_R$  is the (known) non-dimensional critical reaction temperature, i.e. the temperature at which significant reaction first occurs. The parameter  $\hat{A}_0$  is treated as  $O(1)$ . The reaction temperature will later be used to identify a reaction time scale  $t_R$ . As in high activation energy asymptotic analyses (e.g. [35]), the small parameter  $\varepsilon$ , non-dimensional activation energy and the critical reaction temperature are related by  $\varepsilon = T_R^2 / \hat{E}$ .

The assumed asymptotic scalings are selected for facilitation of the asymptotic analysis and are qualitatively consistent with data found in the literature [15, 27, 32–34]. In our analysis we consider materials in which onset of significant plastic work and onset of significant reaction occur over similar timescales. These we refer to as “reactive shear bands”. For materials in which localisation of plastic work occurs well before significant reaction (or vice-versa) these relations should be adjusted so that the appropriate dominant plastic or reaction properties are related through different powers of  $\varepsilon$ . The limit considered herein is perhaps the most important to consider when concerned with safety and handling; accidental mechanical stimuli are typically of a short duration and therefore materials which react shortly after the generation of a shear band pose the greatest risk of ignition.

### 3.1 Elastic stage

In the early stages of deformation the plastic strain-rate is initially exponentially small. This remains the case until the stress and temperature have risen sufficiently to make the argument of the exponent in (3.6) positive. Additionally, the Arrhenius source term is exponentially small until the critical reaction temperature  $T_R$  is reached. Thus, for early times the inert elastic solution of (3.1)–(3.2) is given by

$$T_e(y, t) = 1 + \delta \int_0^t \frac{e^{-\frac{y^2}{4(t-t')}}}{[\pi(t-t')]^{1/2}} h(t') dt', \quad (3.8)$$

$$s_e(y, t) = 1 + \omega t, \quad (3.9)$$

see, for example, [36, p.75]. Here the heat flux inhomogeneity is represented as  $q(t) = \delta h(t)$ ,  $0 \leq h(t) \leq 1$ . The scaling of the heat flux is such that  $0 < \varepsilon \ll \delta \ll 1$ , so that  $\delta$  is sufficiently large to introduce localisation, but still small enough to be negligible in comparison with physical factors that control the evolution of the shear band. The ordering of the small parameters has the physical interpretation that the thermal stimulus is sufficiently strong to cause the onset of plastic localisation, but is not so strong that it causes a rapid departure from the elastic response of the material. This early time solution will be used as the basis of our asymptotic analysis.



### 3.2 Onset of Reactive Shear Band

In this section we develop a boundary layer analysis which splits the problem into an elastic stage and a plastic-reactive stage, where the latter simultaneously accounts for heating due to plastic work and reaction. Beyond the critical plastic threshold,  $\dot{\gamma}$  becomes large due to the multiplicative scaling. This motivates the definition of a critical time scale  $t_p$  at which the onset of significant plastic work occurs, i.e. the time at which the exponential in (3.6) becomes  $O(1)$ . Therefore  $t_p$  is defined by the smallest solution of

$$\beta_1[T_p - T_e(0, t_p)] + \beta_2[s_p - s_e(0, t_p)] = 0. \quad (3.10)$$

Given that the stimulus for the shear band is placed along the centreline, the plastic work first becomes significant near  $y = 0$ , and occurs at time  $t = t_p$ . At this stage the solution will be a perturbation of the elastic solution (3.8)–(3.9). The temperature in the shear band will increase due to plastic work, until the critical reaction temperature is reached. As previously discussed, we consider the case where the subsequent reaction occurs on a similar timescale to the growth of the plastic work term. It is possible to consider a model in which the plastic and reactive behaviour occur on disparate timescales, but we restrict ourselves to the most critical case.

We introduce new independent variables  $\xi$  and  $\tau$  such that

$$y = \varepsilon\xi, \quad t = t_p + \varepsilon\tau, \quad \xi > 0, \quad \tau > -\frac{t_p}{\varepsilon} \rightarrow -\infty, \quad (3.11)$$

which are appropriate to describe the inner solution in the boundary layer near  $y = 0$ , where the localised plastic straining first begins to occur. In order to identify the onset of the reaction we define a critical reaction timescale  $\tau_R$  (related to the “original time” by  $t_R = t_p + \varepsilon\tau_R$ ) as the solution of

$$T_R = T_e(0, t_p + \varepsilon\tau_R) + \varepsilon T_1(0, \tau_R) + o(\varepsilon), \quad (3.12)$$

where the function  $T_1$  is still to be determined as part of the solution.

In the inner layer we expand the temperature and stress in powers of  $\varepsilon$  as

$$T = T_e(\varepsilon\xi, t_p + \varepsilon\tau) + \varepsilon T_1(\xi, \tau) + \varepsilon^{3/2} T_2(\xi, \tau) + \dots, \quad (3.13)$$

$$s = s_e(\varepsilon\xi, t_p + \varepsilon\tau) + \varepsilon s_1(\xi, \tau) + \varepsilon^{3/2} s_2(\xi, \tau) + \dots. \quad (3.14)$$

Physically we expect the solution in the shear band to be driven by plastic work and the chemical reaction. The chosen scalings in the expansion allow for the appropriate balance between the plastic work and reaction terms in the governing equations (3.1)–(3.2). We expand the elastic parts of the solution as

$$T_e(\varepsilon\xi, t_p + \varepsilon\tau) = T_e(0, t_p) + \varepsilon(a\tau - b\xi) + o(\varepsilon), \quad (3.15)$$

$$s_e(\varepsilon\xi, t_p + \varepsilon\tau) = s_e(0, t_p) + \varepsilon\hat{\omega}\tau + o(\varepsilon), \quad (3.16)$$

where

$$a = T_{e_t}(0, t_p) = \delta \int_0^{t_p} [\pi(t_p - t')]^{-1/2} h'(t') dt', \quad b = -T_{e_y}(0, t_p) = \delta h(t_p). \quad (3.17)$$

Substitution of the expansions for the temperature and stress into (3.1)–(3.2) gives

$$\left[ s_1 + \varepsilon^{1/2} s_2 + \dots \right]_\tau = \hat{\rho}_0^{-1} \int_{-\infty}^{\tau} \left[ \varepsilon^{-1} s_1 + \varepsilon^{-1/2} s_2 + \dots \right]_{\xi\xi} d\tau' - \dot{\gamma}, \quad (3.18)$$

$$\left[ T_1 + \varepsilon^{1/2} T_2 + \dots \right]_\tau = \left[ \varepsilon^{-1} T_1 + \varepsilon^{-1/2} T_2 + \dots \right]_{\xi\xi} + \lambda [s_e + \varepsilon s_1 + \dots] \dot{\gamma} + \hat{\Omega} \hat{A} \exp(-\hat{E}/T), \quad (3.19)$$

where the expansion of the plastic strain-rate is given by

$$\dot{\gamma} = \dot{\gamma}_0 \varepsilon^{-1/2} \{ \exp[\beta_4 \tau - \beta_1 b \xi + \beta_1 T_1 + \beta_2 s_1 - \beta_3 \hat{\gamma}] + o(1) \}, \quad (3.20)$$

and where the  $O(1)$  variable  $\hat{\gamma}(\xi, \tau) = \varepsilon^{-1/2} \gamma$  has been introduced. Here  $\beta_4 = \beta_1 a + \beta_2 \hat{\omega} > 0$ , justified by the observation that  $\beta_2 \hat{\omega} > 0$  and  $a \sim O(\delta)$  is negligible. The expansion of the Arrhenius source term is given by

$$\hat{\Omega} \hat{A} \exp(-\hat{E}/T) = \hat{A}_0 \varepsilon^{-1/2} \exp \{ a(\tau - \tau_R) - b \xi + T_1 - T_1(0, \tau_R) + o(1) \}, \quad (3.21)$$

and we observe that the onset of reaction is delayed by the shift in time  $\tau_R$ .

We now solve the sequence of boundary value problems which arise from considering powers of  $\varepsilon$ . At  $O(\varepsilon^{-1})$  we have the problem

$$\int_{-\infty}^{\tau} s_{1\xi\xi} d\tau = 0, \quad s_{1\xi}(0, \tau) = 0, \quad s_1(\xi, -\infty) = 0, \quad (3.22)$$

$$T_{1\xi\xi} = 0, \quad T_{1\xi}(0, \tau) = 0, \quad T_1(\xi, -\infty) = 0. \quad (3.23)$$

Integrating both equations twice with respect to  $\xi$  and applying the boundary conditions at  $\xi = 0$  reveals that the solutions must be functions of time  $\tau$  only:

$$T_1(\xi, \tau) = f_1(\tau), \quad f_1(-\infty) = 0, \quad s_1(\xi, \tau) = g_1(\tau), \quad g_1(-\infty) = 0, \quad (3.24)$$

where  $f_1(\tau)$  and  $g_1(\tau)$  are to be determined by matching with the outer solution. We next solve the problem at  $O(\varepsilon^{-1/2})$ :

$$\int_{-\infty}^{\tau} s_{2\xi\xi} d\tau = \hat{\rho}_0 \dot{\gamma}_0 \exp[\beta_4 \tau - \beta_1 b \xi + \beta_1 f_1 + \beta_2 g_1], \quad (3.25)$$

$$s_{2\xi}(0, \tau) = 0, \quad s_2(\xi, -\infty) = 0, \quad (3.26)$$

$$\begin{aligned} T_{2\xi\xi} = & -\lambda \dot{\gamma}_0 (1 + \hat{\omega} t_p) \exp[\beta_4 \tau - \beta_1 b \xi + \beta_1 f_1 + \beta_2 g_1 - \beta_4 \hat{\gamma}] \\ & - \hat{A}_0 \exp[a(\tau - \tau_R) - b \xi + f_1(\tau) - f_1(\tau_R)], \end{aligned} \quad (3.27)$$

$$T_{2\xi}(0, \tau) = 0, \quad T_2(\xi, -\infty) = 0. \quad (3.28)$$

This has solution

$$\begin{aligned} s_2(\xi, \tau) = & \frac{\hat{\rho}_0 \dot{\gamma}_0}{\beta_1 b} \left( \xi \exp(-\beta_3 \hat{\gamma}(0, \tau)) + \frac{\exp(-\beta_1 b \xi - \beta_3 \hat{\gamma})}{\beta_1 b} \right. \\ & \left. + \beta_3 \int_0^\xi \frac{\exp(-\beta_1 b \xi - \beta_3 \hat{\gamma})}{\beta_1 b} \hat{\gamma}_\xi d\xi - \beta_3 \int_0^\xi \int_0^\xi \exp(-\beta_1 b \xi - \beta_3 \hat{\gamma}) \hat{\gamma}_\xi d\xi d\xi \right) \end{aligned}$$

$$\begin{aligned}
& \times \frac{d}{d\tau} \{ \exp[\beta_4\tau + \beta_1 f_1(\tau) + \beta_2 g_1(\tau)] \} \\
& - \hat{\rho}_0 \dot{\gamma}_0 \beta_3 \int_0^\xi \int_0^\xi \exp(-\beta_1 b\xi - \beta_3 \hat{\gamma}) \hat{\gamma}_\tau d\xi d\xi \times \exp[\beta_4\tau + \beta_1 f_1(\tau) + \beta_2 g_1(\tau)] \\
& + g_2(\tau), \quad g_2(-\infty) = 0,
\end{aligned} \tag{3.29}$$

$$\begin{aligned}
T_2(\xi, \tau) = & -\frac{\lambda \dot{\gamma}_0 (1 + \hat{\omega} t_p)}{\beta_1 b} \left( \xi \exp(-\beta_3 \hat{\gamma}(0, \tau)) + \frac{\exp(-\beta_1 b\xi - \beta_3 \hat{\gamma})}{\beta_1 b} \right. \\
& + \beta_3 \int_0^\xi \frac{\exp(-\beta_1 b\xi - \beta_3 \hat{\gamma})}{\beta_1 b} \hat{\gamma}_\xi d\xi - \beta_3 \int_0^\xi \int_0^\xi \exp(-\beta_1 b\xi - \beta_3 \hat{\gamma}) \hat{\gamma}_\xi d\xi d\xi \Big) \\
& \times \exp[\beta_4\tau + \beta_1 f_1(\tau) + \beta_2 g_1(\tau)] + f_2(\tau), \quad f_2(-\infty) = 0,
\end{aligned} \tag{3.30}$$

where the functions  $f_2(\tau)$  and  $g_2(\tau)$  are to be determined.

In order to satisfy the boundary conditions away from the shear band we consider an outer layer, in which the appropriate independent variables are

$$y = \varepsilon^{1/2} Y, \quad t = t_p + \varepsilon \tau, \quad Y > 0, \quad \tau > -\frac{t_p}{\varepsilon} \rightarrow -\infty. \tag{3.31}$$

In this region both the plastic straining and reaction are negligible. Motivated by achieving a balance between the time derivative and diffusive terms in the governing equations [8], we introduce the expansions

$$T = T_e(\varepsilon^{1/2} Y, t_p + \varepsilon \tau) + \varepsilon T_1^O(Y, \tau) + \varepsilon^{3/2} T_2^O(Y, \tau) + \dots, \tag{3.32}$$

$$s = s_e(\varepsilon^{1/2} Y, t_p + \varepsilon \tau) + \varepsilon s_1^O(Y, \tau) + \varepsilon^{3/2} s_2^O(Y, \tau) + \dots. \tag{3.33}$$

For the analysis here we only require the leading-order governing equations in the outer layer, which read

$$s_{1\tau}^O = \hat{\rho}_0^{-1} \int_{-\infty}^\tau s_{1Y}^O d\tau', \quad s_1^O(\infty, \tau) = 0, \quad s_1^O(Y, -\infty) = 0, \tag{3.34}$$

$$T_{1\tau}^O = T_{1Y}^O, \quad T_1^O(\infty, \tau) = 0, \quad T_1^O(Y, -\infty) = 0. \tag{3.35}$$

No boundary conditions are imposed at  $Y = 0$ . Instead we must perform an asymptotic matching between the inner and outer solutions. The inner expansion is expressed in terms of the outer variables and equated to the outer expansion in order to derive matching relations at  $Y = 0$ . This process provides the boundary conditions

$$T_1^O(0, \tau) = f_1(\tau), \quad s_1^O(0, \tau) = g_1(\tau), \tag{3.36}$$

$$\begin{aligned}
T_{1Y}^O(0, \tau) = & -\frac{\lambda \dot{\gamma}_0 (1 + \hat{\omega} t_p)}{\beta_1 b} \exp(\beta_4\tau + \beta_1 f_1(\tau) + \beta_2 g_1(\tau) - \beta_3 \hat{\gamma}(0, \tau)) \\
& - \frac{\hat{A}_0}{b} \exp(a(\tau - \tau_R) + f_1(\tau) - f_1(\tau_R)),
\end{aligned} \tag{3.37}$$

$$s_{1Y}^O(0, \tau) = \frac{\hat{\rho}_0 \dot{\gamma}_0}{\beta_1 b} \frac{d}{d\tau} \exp(\beta_4\tau + \beta_1 f_1(\tau) + \beta_2 g_1(\tau) - \beta_3 \hat{\gamma}(0, \tau)). \tag{3.38}$$

Solution of equations (3.34)–(3.35) subject to the boundary conditions (3.37)–(3.38) provides

$$s_1^O(Y, \tau) = -\frac{\hat{\rho}_0^{1/2}\dot{\gamma}_0}{\beta_1 b} \times \exp \left[ \beta_4(\tau - \hat{\rho}_0^{1/2}Y) + \beta_1 f_1(\tau - \hat{\rho}_0^{1/2}Y) \right. \\ \left. + \beta_2 g_1(\tau - \hat{\rho}_0^{1/2}Y) - \beta_3 \hat{\gamma}(0, \tau - \hat{\rho}_0^{1/2}Y) \right], \quad (3.39)$$

$$T_1^O(Y, \tau) = \int_{-\infty}^{\tau} \left\{ \frac{\lambda \dot{\gamma}_0(1 + \hat{\omega}t_p)}{\beta_1 b} \exp [\beta_4 \tau' + \beta_1 f_1(\tau') + \beta_2 g_1(\tau') - \beta_3 \hat{\gamma}(0, \tau')] \right. \\ \left. + \frac{\hat{A}_0}{b} \exp[a(\tau - \tau_R) + f_1(\tau) - f_1(\tau_R)] \right\} \times \exp \left[ -\frac{Y^2}{4(\tau - \tau')} \right] \frac{d\tau'}{[\pi(\tau - \tau')]^{1/2}}. \quad (3.40)$$

Imposing matching conditions between the inner and outer solution at  $Y = 0$  gives a pair of coupled nonlinear equations for the leading-order temperature and stress perturbations in the shear band, namely

$$f_1(\tau) = \int_{-\infty}^{\tau} \left\{ \frac{\lambda \dot{\gamma}_0(1 + \hat{\omega}t_p)}{\beta_1 b} \exp [\beta_4 \tau' + \beta_1 f_1(\tau') + \beta_2 g_1(\tau') - \beta_3 \hat{\gamma}(0, \tau')] \right. \\ \left. + \frac{\hat{A}_0}{b} \exp[a(\tau - \tau_R) + f_1(\tau) - f_1(\tau_R)] \right\} \frac{d\tau'}{[\pi(\tau - \tau')]^{1/2}}, \quad (3.41)$$

$$g_1(\tau) = -\frac{\hat{\rho}_0^{1/2}\dot{\gamma}_0}{\beta_1 b} \exp [\beta_4 \tau + \beta_1 f_1(\tau) + \beta_2 g_1(\tau) - \beta_3 \hat{\gamma}(0, \tau)], \quad (3.42)$$

with the scaled centreline plastic strain given by

$$\hat{\gamma}(0, \tau) = \int_{-\infty}^{\tau} \dot{\gamma}_0 \exp [\beta_4 \tau' + \beta_1 f_1(\tau') + \beta_2 g_1(\tau') - \beta_3 \hat{\gamma}(0, \tau')] d\tau'. \quad (3.43)$$

These are to be solved in conjunction with (3.12) in order to determine the critical reaction time  $\tau_R$ . We note that  $f_1(\tau) \geq 0$  and  $g_1(\tau) \leq 0$  which is consistent with the physical observation that plastic deformation leads to an increase in the temperature and a decrease in the stress [8]. In particular, rapid growth (decay) of the temperature (stress) is associated with the formation of a shear band.

## 4 Reactive Shear Band criterion

In order to analyse the coupled equations for the reactive shear bands (3.41)–(3.43) we introduce the new variables

$$f(\eta) = \beta_1 f_1(\tau), \quad g(\eta) = -\beta_2 g_1(\tau), \quad k(\eta) = \beta_3 \hat{\gamma}(0, \tau), \quad \eta = \beta_4 \tau + \log \left[ \frac{\lambda \dot{\gamma}_0(1 + \hat{\omega}t_p)}{b\beta_4^{1/2}} \right],$$

to re-write the problem on the  $\eta$  timescale. This introduces the non-dimensional parameters

$$\Lambda_p = \frac{\beta_2(\hat{\rho}_0\beta_4)^{1/2}}{\beta_1\lambda(1 + \hat{\omega}t_p)}, \quad \Lambda_k = \frac{\beta_3 b}{\lambda(1 + \hat{\omega}t_p)}, \quad \Lambda_R = \frac{\hat{A}_0}{b\beta_4^{1/2}}, \quad \Lambda_t = \frac{a}{\beta_4}, \quad (4.1)$$

which are known in terms of the material properties and applied shearing motion. Now (3.41)–(3.43) take the simplified form

$$f(\eta) = \int_{-\infty}^{\eta} [\pi(\eta - \eta')]^{-1/2} \left\{ \exp[\eta' + f(\eta') - g(\eta') - k(\eta')] \right. \quad (4.2)$$

$$\left. + \Lambda_R \exp[\Lambda_t(\eta' - \eta'_R) + \beta_1^{-1}(f(\eta') - f(\eta'_R))] \right\} d\eta', \quad (4.3)$$

$$g(\eta) = \Lambda_p \exp[\eta + f(\eta) - g(\eta) - k(\eta)], \quad (4.4)$$

$$k(\eta) = \Lambda_k \int_{-\infty}^{\eta} \exp[\eta' + f(\eta') - g(\eta') - k(\eta')] d\eta', \quad (4.5)$$

and correspond to the magnitudes of the perturbations to the temperature, stress and strain hardening variable, respectively. The parameters  $\Lambda_p$ ,  $\Lambda_k$  and  $\Lambda_t$  relate to the material properties, applied shearing motion and heat flux inhomogeneity, whereas the parameter  $\Lambda_R$  relates to the properties of the chemical reaction.

For the special case  $\Lambda_p = 1$  and  $\Lambda_k, \Lambda_R = 0$  we have the exact solution  $f(\eta) = g(\eta) = e^\eta$  and  $k(\eta) = 0$  for all values of  $\Lambda_t$ . For other parameter values we investigate the behaviour of  $f(\eta)$ ,  $g(\eta)$  and  $k(\eta)$  numerically using Newton's method. In particular, we are interested in understanding how the inclusion of a chemical reaction in the model affects the tendency for a shear band to form when compared with the inert solution. In [8] a shear band criterion is developed by adopting the position that the perturbations should remain  $O(1)$  at the critical plastic time for plastic work  $t = t_p$  ( $\tau = 0$ ). For the parameter values quoted in [8] it is found that  $\tau = 0$  corresponds to  $\eta \sim 1$  to 7. For  $\Lambda_p < 10$  the perturbations become  $O(10)$  at time  $\eta \sim 7$ , and it is argued that  $\Lambda_p < 10$  provides a useful threshold below which the formation of shear bands occurs. In the following we will assume that the parameters which appear in the definition of  $\eta$  are such that  $\eta = 7$  corresponds to  $\tau = 0$ . This will allow for a direct comparison between the inert results in [8] and our reactive shear band model.

In order to simplify the analysis to follow we note that  $\beta_1 \sim O(1)$ , and through an appropriate choice of scaling we can always set  $\beta_1 = 1$ . Further, we note that the parameter  $\Lambda_t = a/(\beta_1 a + \beta_2 \hat{\omega}) \sim O(\delta)$ . Numerical investigation shows that the effect of varying  $\Lambda_t$  between 0 and 0.1 is minimal, so in the interest of simplicity we set  $\Lambda_t = 0$  and study the reduced three parameter system controlled by  $\Lambda_p$ ,  $\Lambda_k$  and  $\Lambda_R$ . In Figures 3 and 4 we give results for a range of parameter values. In particular we consider  $0 < \Lambda_p \leq 100$ , which allows for a direct comparison with the results in [8]. It should be noted that even though the analysis was carried out treating the various parameters which make up  $\Lambda_p$  as  $O(1)$ , numerical investigations reveal that the asymptotic solution shows good agreement with the full model for large values of  $\Lambda_p$ .

Figure 3 shows a series of numerically computed results for the inert case  $\Lambda_R = 0$ , allowing the influence of the strain hardening parameter  $\Lambda_k$  to be more clearly observed. Panels (a)–(c) show the perturbations to the centreline temperature  $f(\eta)$ , stress  $g(\eta)$  and strain hardening variable  $k(\eta)$  in the absence of any hardening, and are exactly those given in [8]. As  $\Lambda_k$  is increased we observe that the growth of the centreline temperature and stress is slowed, particularly for the results with  $\Lambda_p < 10$ , and it is argued that the inclusion of strain hardening effects can prevent the rapid growth (decay) of temperature (stress) typically associated with shear banding. Assuming the same parameter values as used in [8], we may say that for sufficiently strong strain hardening effects ( $\Lambda_k \geq 1$ ) the formation of a shear band may be suppressed: in panels (g) and (h) we see

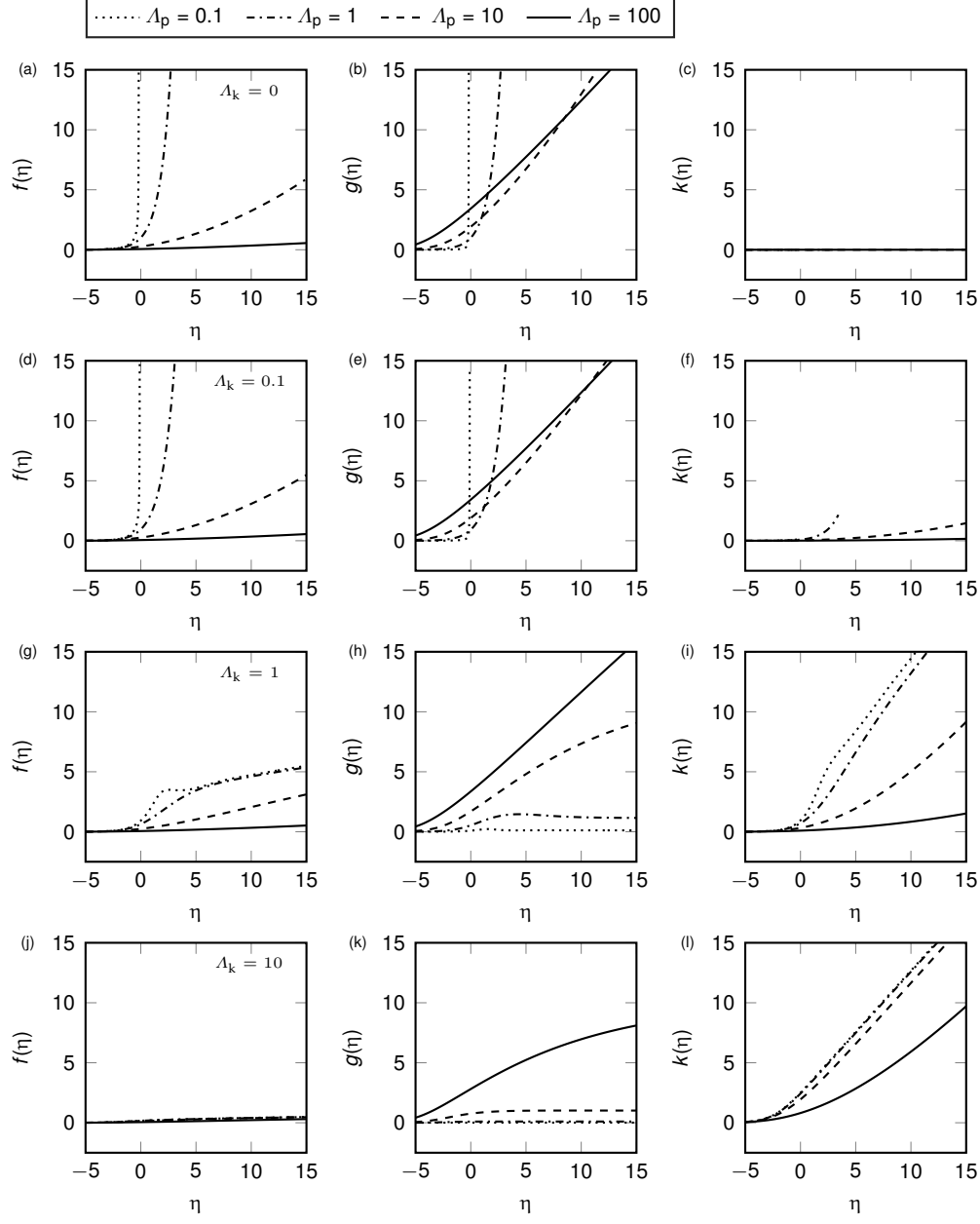


**Figure 3:** Results for the non-reactive case  $\Lambda_R = 0$  and hardening parameter  $\Lambda_k = 0, 0.1, 1$ , and  $10$ , top to bottom, respectively. In each panel results are given for  $\Lambda_p = 0.1$  ( $\cdots$ ),  $1$  ( $- \cdot -$ ),  $10$  ( $- -$ ) and  $100$  ( $-$ ).

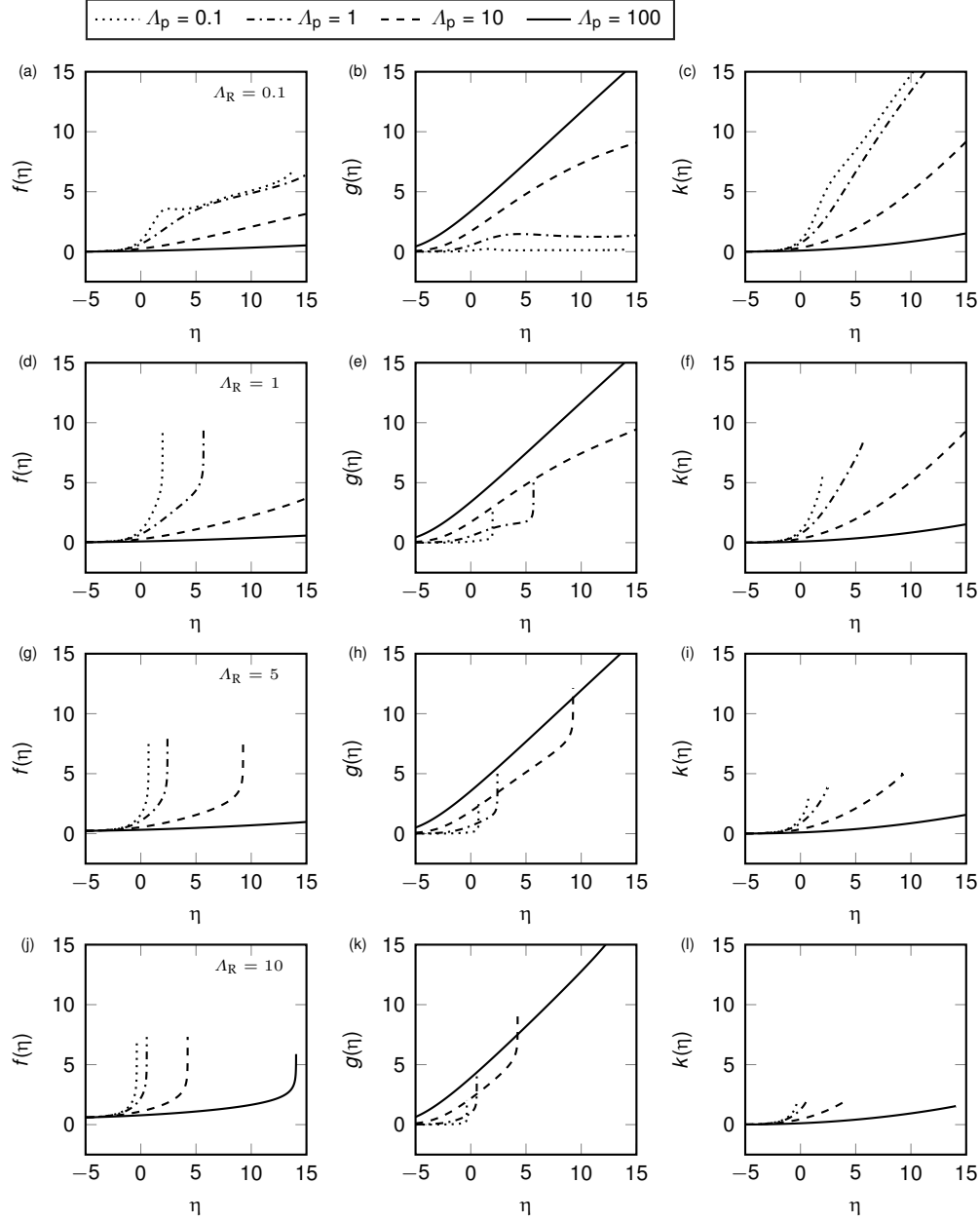
that the perturbations to the temperature and stress remain  $O(1)$  at time  $\eta = 7$  for all values of  $\Lambda_p$ .

Figure 4 shows numerical results with fixed hardening parameter  $\Lambda_k = 1$  and increasing reaction parameter  $\Lambda_R = 0.1, 1, 5$ , and  $10$ , from top to bottom, respectively. It is clear to observe that increasing  $\Lambda_R$ , which corresponds to increasing reaction rate or heat of reaction, causes the perturbations to the temperature and stress to grow more rapidly, thus triggering the earlier onset of shear banding behaviour. In fact, through the addition of a chemical reaction, the model gives rise to the formation of shear bands for parameter values for which a shear band would not be observed in an inert material. For instance, in Figure 3 (g) we see that for all values of  $\Lambda_p$  there is only a moderate increase in the perturbation to the temperature and  $f(\eta)$  remains  $O(1)$  for the times shown. However, the corresponding result with  $\Lambda_R = 1$ , shown in Figure 4 (d), depicts rapid growth  $\Lambda_p = 0.1$  and  $1$ , indicative of the onset of shear banding.

Figure 5 shows the outcome of a number of simulations in the  $\Lambda_p - \Lambda_R$  plane, with  $\Lambda_k = 0, 0.1, 10$ , and  $1$ . In the figure, triangles indicate that a shear band did not form, i.e. the perturbations remained  $O(1)$  at the critical plastic time  $t = t_p$ . Circles indicate that the perturbations to the temperature and stress were no longer  $O(1)$  at time  $t_p$ , and therefore a shear band did form. As discussed in [8], for  $\Lambda_p < 10$  a shear band is always initiated in the absence of hardening, irrespective of the reaction properties. However, the reaction may affect the growth rate of the temperature and stress perturbations once the band has formed. For  $\Lambda_p > 10$  a shear band is not observed when there is no reaction, but it is found that a shear band may be initiated by sufficiently increasing  $\Lambda_R$ . That is, for a sufficiently strong, or fast, reaction a shear band may be initiated in a material which would not otherwise undergo shear banding under the same load. In Figure 5 (a) we initially observe that as  $\Lambda_p$  is increased a greater value of  $\Lambda_R$  is required in order to initiate a shear band. However, for  $\Lambda_p$  large enough ( $\Lambda_p > 70$ ) we see that the critical value of  $\Lambda_R$  required for shear band formation begins to decrease. This is best understood by referring back to Figure 3 (a,b), which shows the corresponding inert results. We see that the stress perturbation  $g(\eta)$  grows more slowly as  $\Lambda_p$  is increased from  $0.1$  through to  $10$ , but begins to grow more rapidly again for  $\Lambda_p = 100$ . When we introduce the chemical reaction, the effects of thermal softening are increased which causes  $g(\eta)$  to increase at an even faster rate, triggering the formation of a shear band. Interestingly, we see that increasing  $\Lambda_k$  increases the size of the region in parameter space where no shear band is observed and for  $\Lambda_k = 10$ , shown in Figure 5 (d), it is found that a shear band is prevented entirely until the reaction parameter is increased significantly ( $\approx \Lambda_R > 6$ ). This highlights the important role strain hardening may play in the development of shear bands.

## 5 Comparison with full numerical solution and approximate theories

In order to solve the full system of governing equations (2.13)–(2.17) numerically, we adapt the so-called “cohesive” scheme in [7] to include heating due to a chemical reaction. Here we give a brief description of the numerical method, and refer the reader to [7] for the full details. The spatial domain  $-1 \leq y \leq 1$  is discretised into  $N$  segments of equal length  $\Delta y = 1/N$ , and the integration time step is fixed as  $\Delta t = \Delta y/S$ , where  $S = \sqrt{1/\hat{\rho}}$  is the non-dimensional elastic wave speed. Thus, the  $y-t$  plane is divided into a rectangular mesh, with each of the nodes being linked by the characteristic lines  $dy/dt = S, -S, 0$ . First, the temperature is assumed known, and the mechanical equations (2.13) and (2.15), along with the constitutive laws (2.16) and (2.17), are solved via an iterative Newton-Raphson scheme. These variables, along with the known



**Figure 4:** Results for the reactive case with  $\Lambda_R = 0.1, 1, 5$ , and  $10$ , top to bottom, respectively, and fixed hardening parameter  $\Lambda_K = 1$ . In each panel results are given for  $\Lambda_p = 0.1$  ( $\cdots$ ),  $1$  ( $\cdots$ ),  $10$  ( $-$ ) and  $100$  ( $-$ ).



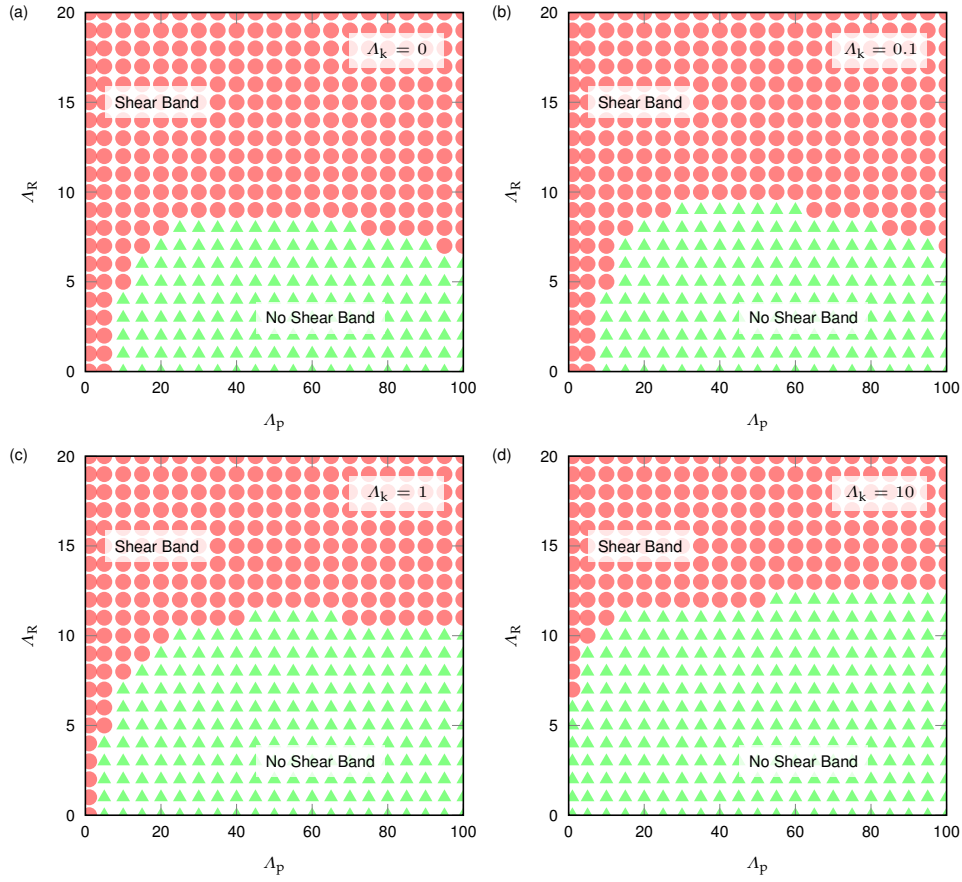


**Figure 5:** A sketch of the region in the  $\Lambda_P - \Lambda_R$  plane in which a shear band is formed, for values: (a)  $\Lambda_k = 0$ ; (b)  $\Lambda_k = 0.1$ ; (c)  $\Lambda_k = 1$ ; and (d)  $\Lambda_k = 10$ . Triangles indicate that no shear band was formed, whereas circles indicate a shear band was formed, based on the criterion that the perturbations remain  $O(1)$  at the critical time  $\tau = 0$ , as originally discussed in [8].

temperature  $T$ , may be used to compute the plastic strain  $\gamma$  and strain-rate  $\dot{\gamma}$ . With all mechanical variables regarded as known, we advance equation (2.14) forward in time. For the inert problem, it is claimed that, due to the smoothness of thermal diffusion compared with stress wave propagation, the decoupled approach gives accurate results provided the mechanical step can be solved accurately [7]. In order to accurately capture the rapid heating due to the chemical reaction we iterate the computation between the mechanical and thermal stage. This approach gives satisfactory results provided that the integration timestep is sufficiently small. Typically we found  $\Delta t \sim 10^{-4}$  was sufficient.

The resulting mechanical finite-difference equations to be solved on the interior of the domain are

$$s_i^{t+\Delta t} = \frac{s_{i-1}^t + s_{i+1}^t}{2} + \frac{\hat{\rho}S}{2} [v_{(i+1)-}^t - v_{(i-1)+}^t] - \frac{\hat{\rho}S\Delta y}{2} \dot{\gamma}_i^{t+\Delta t}, \quad (5.1)$$

$$\dot{\gamma}_i^{t+\Delta t} = \dot{\gamma}(s_i^{t+\Delta t}, T_i^t, \gamma_i^{t+\Delta t}), \quad (5.2)$$

$$\gamma_i^{t+\Delta t} = \gamma_i^t + \frac{\Delta t}{2} [\dot{\gamma}_i^{t+\Delta t} + \dot{\gamma}_i^t]. \quad (5.3)$$

Once the mechanical equations have converged, the thermal part of the problem is solved using a discretised version of (2.14):

$$\begin{aligned} T_i^{t+\Delta t} = T_i^t + \Delta t \left( \frac{T_{i+1}^t - 2T_i^t + T_{i-1}^t}{\Delta y^2} \right) + \Delta t \lambda \left( \frac{s_i^t + s_i^{t+\Delta t}}{2} \right) \left( \frac{\dot{\gamma}_i^t + \dot{\gamma}_i^{t+\Delta t}}{2} \right) \\ + \Delta t \hat{\Omega} \hat{A} \exp \left( -\frac{2\hat{E}}{T_i^t + T_i^{t+\Delta t}} \right). \end{aligned} \quad (5.4)$$

The above equation, which uses a second order midpoint rule for the heat generation terms, is iterated with the mechanical part of the problem until the temperature has converged. In the early stages of the problem, this iteration stage is not required since the temperature changes on a timescale much shorter than the timescale required by the mechanical part of the scheme. However, as the temperature is increased the heating due to reaction becomes important, and the updated value of the temperature may be used to solve an updated version of the mechanical equations (5.1)–(5.3). Such an iteration process is repeated until a solution is obtained to within a specified tolerance. Equations (5.1)–(5.4) are supplemented by appropriate boundary conditions, see [7].

Figure 6 shows a comparison of the centreline temperature stress as predicted by the asymptotic and numerical results with (a,b) and without (c,d) the effect of strain hardening. The boundary layer analysis developed in Section 3, labelled ‘Asymptotic’, provides an excellent agreement with the numerical results obtained using the cohesive scheme described in [7]. We observe that the key features of the shear banding behaviour are well-predicted by the asymptotic solution, in particular we see the characteristic drop in stress associated with shear band formation. For the results which include strain hardening we observe that the drop in stress is less rapid and the formation of the shear band is delayed, in agreement with the conclusions of our asymptotic analysis that strain hardening delays the shear banding process.

Also shown are the results from two approximate theories: one in which the reaction is assumed exponentially small in the initial stages of shear band formation (Approximation I); and another, motivated by the Thermal Explosion Theory [15], in which the heating is first dominated by plastic work, and then “switches over” to being dominated by chemical reaction at the induction time  $t^*$  (Approximation II).

In Approximation I, the problem is split into three stages: an elastic stage; a plastic stage; and a plastic-reactive stage. The plastic stage problem is first solved using boundary-layer techniques, similar in fashion to the solution in Section 3, but with  $\hat{A}_0 = 0$ . This is consistent with our assumption that the plastic work dominates until the critical reaction temperature  $T_R$  is reached. We then introduce a new timescale  $\hat{\tau}$  through the relation  $t = t_p + \varepsilon(\tau_R + \varepsilon^{1/2}\hat{\tau})$  which is suitable to describe the solution once the reaction has commenced. During this final reaction stage, the model accounts for heating due to plastic work and chemical reaction, and the solution is given by

$$T = T_R + \varepsilon\theta(\xi, \hat{\tau}) + o(\varepsilon), \quad (5.5)$$

$$s = s_R + \varepsilon\psi(\xi, \hat{\tau}) + o(\varepsilon), \quad (5.6)$$

where  $s_R$  is the stress at the time at which the critical reaction temperature  $T_R$  is reached. The corrections to the temperature and stress are governed by a system of two coupled ordinary differential equations

$$\theta_{\hat{\tau}} = \lambda s_R \dot{\gamma}_0 \exp\{\beta_3 \tau_R + \beta_1 T_1(\tau_R) + \beta_2 s_1(\tau_R) + \beta_3 \hat{\gamma}(0, \tau_R) + \beta_1 \theta + \beta_2 \psi\} + \hat{A}_0 \exp\{\theta\}, \quad (5.7)$$

$$\psi_{\hat{\tau}} = -\dot{\gamma}_0 \exp\{\beta_3 \tau_R + \beta_1 T_1(\tau_R) + \beta_2 s_1(\tau_R) + \beta_1 \theta + \beta_2 \psi\}, \quad (5.8)$$

along with the initial conditions  $\theta(-\infty) = 0$  and  $\psi(-\infty) = 0$ . Note that the strain appears constant to leading order in the law for the strain-rate, that is the effect of strain hardening appears to be independent of time on the reaction time scale  $\hat{\tau}$ .

The second approximate approach identifies three distinct periods: an induction stage, during which spatially homogenous plastic work induces a temperature rise sufficient to trigger a significant reaction; a reaction period; and a post-reaction period. In contrast to our critical reaction time  $t_R$ , the Thermal Explosion Theory identifies an induction time  $t^*$  corresponding to the time at which heating due to plastic work and reaction become comparable. The reaction stage, during which heating due to plastic work is assumed negligible, commences at time  $t = t^*$ . Using the idea of [15], we use our inert ( $\hat{A}_0 = 0$ ) centreline solution from Section 3, given by  $T_I(t; \tau) = T_e(0, t) + \varepsilon f_1(\tau; \hat{A}_0 = 0)$  and  $s_I(t; \tau) = s_e(0, t) + \varepsilon g_1(\tau; \hat{A}_0 = 0)$ , where the subscript  $I$  denotes inert, to find an induction time  $t^*$ . This is found as the root of

$$\begin{aligned} & \lambda s_I(t^*) \dot{\gamma}_0 \exp\{-\varepsilon^{-1}[\beta_1(T_p - T_I(t^*)) + \beta_2(s_p - s_I(t^*))] - \varepsilon^{-1/2}\beta_3\gamma_I(0, t^*)\} \\ & = \hat{A}_0 \exp\left(\frac{\hat{E}}{T_R} - \frac{\hat{E}}{T_I(t^*)}\right). \end{aligned} \quad (5.9)$$

As in the approximate Thermal Explosion Theory [15], we assume a spatially homogenous solution during the reaction stage. The plastic work term is treated as negligible so that the temperature at the centre of the band is governed by the ordinary differential equation

$$T_t = \hat{\Omega} \hat{A} \exp\left(-\hat{E}/T\right), \quad T(t^*) = T_I(t^*), \quad (5.10)$$

which accounts solely for the heating due to reaction along the centre of the shear band. We further assume

a uniform strain-rate during the reaction stage which gives a strain that depends linearly on time [15]

$$\dot{\gamma}(y, t) \approx \dot{\gamma}^*, \quad \gamma(y, t) \approx \dot{\gamma}^*(t - t^*) + \gamma_I(t^*), \quad (5.11)$$

where the representative strain-rate  $\dot{\gamma}^* = \dot{\gamma}(s_I(t^*), T_I(t^*), \gamma_I(t^*))$  is calculated from the constitutive law (3.6). An approximate time history of the stress in the band during the reaction stage may then be computed by rearranging (3.6) to give

$$s(t) = \frac{\beta_1}{\beta_2}(T_p - T) + s_p + \varepsilon^{1/2} \frac{\beta_3}{\beta_2} [\dot{\gamma}^*(t - t^*) + \gamma_I(t^*)] + \frac{\varepsilon}{\beta_2} \log \left( \frac{\dot{\gamma}^*}{\dot{\gamma}_0} \varepsilon^{1/2} \right). \quad (5.12)$$

An important distinction to make between the boundary layer and approximate approaches is that the dominant balance within the band in the asymptotic solution of Section 3 is between heat diffusion, plastic work and reaction. Solution of the problem then comes from matching with an outer region in which the temperature satisfies the usual one-dimensional heat equation with no heat sources. However, in the two approximate solutions there is a dominant balance between the time derivative of the temperature and either the plastic work and reaction in Approximation I, or just the reaction in Approximation II.

The critical plastic time  $t_p$ , critical reaction time  $t_R$ , approximate critical reaction time  $t_{R_a}$  predicted by Approximation I, and induction time  $t^*$  predicted by Approximation II are shown as vertical lines in Figure 6. The critical plastic time  $t_p$  agrees well with the numerical solution, identified as the time at which the solution first differs from the elastic solution by  $O(\varepsilon)$ . This is most clearly observed in the plots of the stress. Further, the time at which significant heating due to reaction occurs is also well predicted, most accurately by our full asymptotic solution. As expected, the boundary layer analysis of Section 3 gives the most rapid rise (drop) in the temperature (stress) since it accounts for both heating due to plastic work and heating due to reaction. The first approximate solution, Approximation I, only accounts for heating due to plastic work up until time  $t_{R_a}$ , at which point a sharp increase in temperature is observed due to the commencement of a rapid chemical reaction. Interestingly, both Approximations I and II predict that the temperature reaches the reaction temperature  $T_R$  at a comparable time in the absence of hardening, see Figure 6 (a,b), so both methods would provide a similar approximation for the time to runaway. This is likely only the case when we consider heating due to plastic work and reaction to be of a comparable size on a comparable timescale, as we do here.

## 6 Conclusion

In this paper we have developed a model for shear bands occurring in reactive materials motivated by the boundary layer analysis of [8]. The analysis allows for the full system of governing equations to be reduced to four coupled equations used to describe the behaviour of the perturbations to the centreline temperature, stress and strain hardening variable, as well as the critical reaction time. It was demonstrated that the asymptotic solution was able to accurately predict all of the key characteristics of the reactive shear banding process, showing excellent agreement with numerical results computed using an adapted version of the scheme described in [7]. In contrast to the inert case with no strain hardening effects, we find that the initiation of shear banding is controlled by four parameters instead of one. The simplified equations allow for the parameter space to be explored, and a criterion for the initiation of shear bands based on known physical

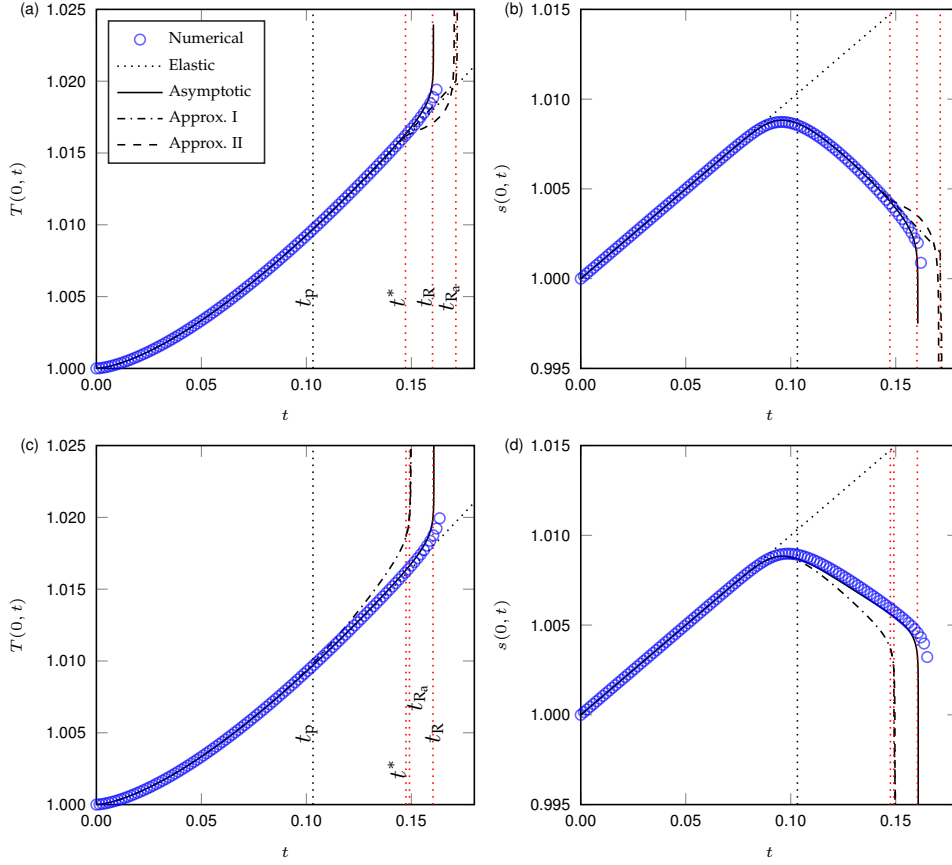


**Figure 6:** Comparison of the centreline temperature and stress as predicted by the asymptotic, approximate and numerical solutions with: (a,b)  $\beta_3 = 0$ ; and (c,d)  $\beta_3 = 0.1$ . In each case the critical plastic time  $t_p$ , critical reaction times  $t_R$  and  $t_{R_a}$ , as well as the induction time  $t^*$  are shown as labelled vertical dotted lines. The parameter values used were  $\hat{\rho}_0 = 10^{-4}$ ,  $\lambda = 10^{-3}$ ,  $\hat{\gamma}_0 = 1$ ,  $\hat{\omega} = 10^{-1}$ ,  $T_p = 1.01$ ,  $s_p = 1.01$ ,  $\hat{A}_0 = 0.05$ ,  $\hat{E} = 10^3$ ,  $T_R = 1.02$ ,  $a = 0.1354$ ,  $b = 0.0395$ ,  $\beta_1 = 1$  and  $\beta_2 = 1$ .

parameters has been suggested. This analysis has extended previous work on shear bands [8], and has identified three new parameters, which will add to the understanding of how localised shearing operates as a hot spot mechanism. As in [8], the dimensionless parameters may be interpreted in terms of physical parameters as follows:

$$\Lambda_p \approx \frac{\rho G \tilde{T}_p (\kappa c \omega)^{1/2}}{P M^{1/2} \tilde{s}_p^{5/2}}, \quad \Lambda_k \approx \delta h(t_p) \frac{\rho c \tilde{T}_p M^{3/2}}{N \tilde{s}_p}, \quad \Lambda_R \approx \frac{\Omega M^{1/2}}{c \tilde{T}_p}, \quad \Lambda_t \approx \frac{a}{\beta_3} \sim \delta \ll 1. \quad (6.1)$$

Unfortunately, the dependence of  $\Lambda_k$  and  $\Lambda_t$  on  $\delta$  cannot be suppressed. However, by relating the small parameter  $\varepsilon$  to the constitutive properties by (3.5), and noting the ordering  $\varepsilon \ll \delta \ll 1$ , one can obtain an estimate of the sizes of both  $\Lambda_k$  and  $\Lambda_t$ .

Unlike other works (e.g. [16, 30, 37]), our analysis gives a parameter-based criterion for shear banding instead of a stress or strain based relation, which is typically related to the maximum of the stress-strain curve [38]. Nonetheless, the results may still be interpreted in the same way: parameter regimes in which a shear band does not form correspond to solutions in which material hardening is predominant; and parameter regimes in which a shear band does form correspond to solutions in which material softening is predominant. One could in principle take the composite solution from the boundary layer analysis presented here to give an explicit solution for use in stress-strain criterion developed in other works, and compare this with experimental results (e.g. [39, 40]), and our parameter-based shear band criterion, but this is beyond the scope of this work.

The usefulness of this analysis is primarily in assessing the tendency of a reactive material to form shear bands, based on its material properties and the shear rate of the deformation. As an example we consider the reactive material LX-14 using the parameter values given in Section 2. By further assuming that  $\tilde{T}_p \approx \tilde{T}_0$  and  $\tilde{s}_p \approx \tilde{s}_0$ , we find that  $\Lambda_p \approx 1.4$  and  $\Lambda_R \approx 10$ , which is well within the range of values for which a shear band would be observed, even in the absence of any reaction. However, if the material were less sensitive to thermal softening, say  $P = 0.1$ , then we would find  $\Lambda_p \approx 14$ . In this case we would not expect a shear band if the material were inert, but we do expect a shear band when we take the reaction into consideration. From this we conclude that considering the behaviour of the reaction can be critical in determining whether or not localised plastic deformation will occur in an explosive material. Since the non-dimensional parameters which govern the behaviour of the perturbations to temperature and stress are known in terms of material properties, the study could be used to inform the manufacture of new explosive materials: for instance, a different binder could be used to alter the bulk material properties in such a way to suppress shear banding.

Of particular practical use is the ability of strain hardening effects to delay the onset of shear banding: it is known that it is possible to control the tendency of a material to exhibit shear banding by altering its strain hardening properties (e.g. [2]). This work predicts that reactive materials are more likely to form shear bands, meaning that strain hardening properties need to be changed considerably more in a reactive material compared to an inert material. In cases where it may not be desirable or practical to alter the mechanical material properties, the analysis presented here reveals the interplay between mechanical and reactive properties, and suggests how altering the properties of the chemical reaction may suppress hot spot mechanisms related to shear banding. Provided the material still performs as intended, choosing an alternative active component (thereby altering the properties of the reaction) may provide an alternative strategy to reduce the susceptibility of a material to shear banding.

In this study it was assumed that the critical temperature for plastic work and reaction were similar in magnitude, so that the reaction occurs soon after the band has formed. In fact, the scalings are such that the onset of significant plastic work and onset of reaction effectively occur simultaneously. In reality, this may not be the case and some adjustment to the analysis would be required. For the case where reaction occurs before significant plastic work (i.e. reactive materials which do not exhibit significant shear localisation) it can be shown that the problem reduces to that of [28]. In this instance the reaction is confined to a thin zone around the centreline, and the problem is effectively equivalent to the heating of a half-space of material with the boundary layer playing the role of a thermal flux applied at the boundary. On the other hand, if the reaction is weak enough it may be observed that the shear band becomes fully developed before the reaction occurs. Solution of this problem would require imposing initial conditions consistent with those found inside a developed shear band and looking for a perturbation about the critical reaction temperature.

**Computational Solution.** The code used to generate the results in this paper can be found in the online repository <https://github.com/rtimms/ReactiveShearBands>

**Data Accessibility.** This article has no additional data.

**Authors Contributions.** All authors have contributed equally to the paper.

**Competing Interests.** The authors have no competing interests.

**Funding.** This work was supported by an EPSRC industrial CASE partnership with AWE [grant number EP/L505729/1].

**Acknowledgements.** The authors would like to thank John Curtis of AWE for helpful discussions.

## References

- [1] Bai Y, Dodd B. 1992 Adiabatic Shear Localization: Occurrence, Theories, and Applications. *Pergamon Press, Oxford, UK*.
- [2] Wright T. 2002 *The physics and mathematics of adiabatic shear bands*. Cambridge University Press, Cambridge, UK.
- [3] Gioia G, Ortiz M. 1996 The Two-Dimensional Structure of Dynamic Boundary Layers And Shear Bands in Thermoviscoplastic Solids. *Journal of the Mechanics and Physics of Solids* **44**, 251–292.
- [4] Edwards D, French D. 1998 Asymptotic and computational analysis of large shear deformations of a thermoplastic material. *SIAM Journal on Applied Mathematics* **59**, 700–724.
- [5] Wright T, Walter J. 1987 On stress collapse in adiabatic shear bands. *Journal of the Mechanics and Physics of Solids* **35**, 701–720.
- [6] Wright T. 1990 Approximate analysis for the formation of adiabatic shear bands. *Journal of the Mechanics and Physics of Solids* **38**, 515–530.
- [7] Zhou F, Wright T, Ramesh K. 2006 A numerical methodology for investigating the formation of adiabatic shear bands. *Journal of the Mechanics and Physics of Solids* **54**, 904–926.
- [8] DiLellio J, Olmstead W. 1997 Shear band formation due to a thermal flux inhomogeneity. *SIAM Journal on Applied Mathematics* **57**, 959–971.

- [9] DiLellio J, Olmstead W. 1997 Temporal evolution of shear band thickness. *Journal of the Mechanics and Physics of Solids* **45**, 345–359.
- [10] Anand L, Gu C. 2000 Granular materials: constitutive equations and strain localization. *Journal of the Mechanics and Physics of Solids* **48**, 1701 – 1733.
- [11] Puzrin A, Germanovich L. 2005 The growth of shear bands in the catastrophic failure of soils. *Proceedings of the Royal Society A: Mathematical, Physical and Engineering Sciences* **461**, 1199–1228.
- [12] Borja RI, Song X, Rechenmacher AL, Abedi S, Wu W. 2013 Shear band in sand with spatially varying density. *Journal of the Mechanics and Physics of Solids* **61**, 219 – 234.
- [13] Song X, Wang K, Ye M. 2018 Localized failure in unsaturated soils under non-isothermal conditions. *Acta Geotechnica* **13**, 73–85.
- [14] Dienes J. 1986 On reactive shear bands. *Physics Letters A* **118**, 433–438.
- [15] Powers J. 1999 Thermal explosion theory for shear localizing energetic solids. *Combustion Theory and Modelling* pp. 103–122.
- [16] Caspar R, Powers J, Mason J. 1998 Investigation of reactive shear localization in energetic solids. *Combustion Science and Technology* **136**, 349–371.
- [17] Boyle V, Frey R, Blake O. 1989 Combined pressure shear ignition of explosives. In *9th Symposium (International) on Detonation* p. 3. Office of Naval Research.
- [18] Chen H, Nesterenko V, LaSalvia J, Meyers M. 1997 Shear-induced exothermic chemical reactions. *Le Journal de Physique IV* **7**, C3–27.
- [19] Frey R. 1980 The initiation of explosive charges by rapid shear. Technical report DTIC Document.
- [20] Howe P, Gibbons Jr G, Webber P. 1986 An experimental investigation of the role of shear in initiation of detonation by impact. Technical report DTIC Document.
- [21] Afanas’ev G, Bobolev V. 1971 *Initiation of solid explosives by impact*. Israel Program for Scientific Translations.
- [22] Field J, Swallowe G, Heavens S. 1982 Ignition Mechanisms of Explosives during Mechanical Deformation. *Proc. R. Soc. Lond. A* **382**, 231–244.
- [23] Williamson D et al.. 2008 Temperature–time response of a polymer bonded explosive in compression (EDC37). *J. Physics D: Applied Physics* **41**, 085404.
- [24] Field J, Bourne N, Palmer S, Walley S, Sharma J, Beard B. 1992 Hot-Spot Ignition Mechanisms for Explosives and Propellants [and Discussion]. *Phil.Trans. of the R. Soc. Lond. A* **339**, 269–283.
- [25] Frank-Kamenetskii D. 1942 On the mathematical theory of thermal explosions. *Acta Physiocochemica URSS* **16**, 357.



- [26] Caspar R. 1996 *Experimental and numerical study of shear localization as an initiation mechanism in energetic solids*. PhD thesis University of Notre Dame, Indiana, USA.
- [27] Austin R, Barton N, Reaugh J, Fried L. 2015 Direct numerical simulation of shear localization and decomposition reactions in shock-loaded HMX crystal. *Journal of Applied Physics* **117**.
- [28] Olmstead W. 1983 Ignition of a combustible half space. *SIAM Journal on Applied Mathematics* **43**, 1–15.
- [29] Curtis J. 2013 Explosive Ignition due to Adiabatic Shear. In *39th International Pyrotechnics Seminar, Valencia, Spain*.
- [30] Recht R. 1964 Catastrophic thermoplastic shear. *Journal of Applied Mechanics* **31**, 189–193.
- [31] Timms R. 2018 *Mathematical Modelling and Investigation of Explosive Pinch, Friction and Shear Problems*. PhD thesis School of Mathematics, University of East Anglia, Norwich, UK.
- [32] Menikoff R, Sewell T. 2002 Constituent properties of HMX needed for mesoscale simulations. *Combustion Theory and Modelling* **6**, 103–125.
- [33] Sewell T, Bedrov D, Menikoff R, Smith G. 2002 Elastic properties of HMX. In *AIP Conference Proceedings* vol. 620 pp. 399–402. AIP.
- [34] Tappan A, Renlund A, Stachowiak J, Miller J, Oliver M. 2002 Mechanical properties determination by real-time ultrasonic characterization of thermally damaged energetic materials. In *12th Symposium (International) on Detonation* pp. 356–362.
- [35] Linan A, Williams F. 1971 Theory of ignition of a reactive solid by constant energy flux. *Combustion Science and Technology* **3**, 91–98.
- [36] Carslaw H, Jaeger J. 1959 *Conduction of heat in solids*. Oxford Clarendon Press, Oxford, UK.
- [37] Antolovich SD, Armstrong RW. 2014 Plastic strain localization in metals: origins and consequences. *Progress in Materials Science* **59**, 1 – 160.
- [38] Zener C, Hollomon JH. 1944 Effect of strain rate upon plastic flow of steel. *Journal of Applied physics* **15**, 22–32.
- [39] Sagapuram D, Viswanathan K, Trumble KP, Chandrasekar S. 2018 A common mechanism for evolution of single shear bands in large-strain deformation of metals. *Philosophical Magazine* **98**, 3267–3299.
- [40] Sagapuram D, Viswanathan K. 2018 Evidence for Bingham plastic boundary layers in shear banding of metals. *Extreme Mechanics Letters* **25**, 27 – 36.